

physica **p** status **s** solidi **S**

www.interscience.wiley.com

reprints

The collage features five journal covers:

- physica status solidi ^a**: applications and materials science. Editor's Choice: Highly efficient all-nitride phosphor-converted white light emitting diode (Regina Mueller-Mach et al., p. 1727). www.pss-a.com
- physica status solidi ^b**: basic solid state physics. Current Trends in Electronic Structure: Embedding and Linear Scaling Techniques (Thomas Beck, and Eduardo Hernandez). www.pss-b.com
- physica status solidi ^c**: current topics in solid state physics. www.pss-c.com
- physica status solidi ^{rrl}**: rapid research letters. www.pss-rapid.com

WILEY-VCH logo is present on the bottom left of the covers.

Excitonic precursor states in ultrafast pump–probe spectroscopies of surface bands

Branko Gumhalter^{*1}, Predrag Lazić², and Nadja Došlić²

¹ Institute of Physics, 10000 Zagreb, Croatia

² Rudjer Bošković Institute, 10000 Zagreb, Croatia

Received 15 October 2009, revised 12 March 2010, accepted 16 March 2010

Published online 22 June 2010

Keywords electronic states, photoelectron spectra, pump–probe spectroscopy, surfaces and interfaces

* Corresponding author: e-mail branko@ifs.hr, Phone: +385 1 4698 805, Fax: +385 1 4698 889

We discuss the formation and evolution of transient coherent excitonic states induced by ultrashort laser irradiation of metal surfaces supporting the surface and image potential bands (typically the low index surfaces of Cu and Ag). These states, which evolve into the image potential states in the course of screening of primary optically excited electron–hole pair, may play the role of early intermediate states in pump–probe spectroscopies of surfaces (e.g. two-photon-photoemission or

sum-frequency generation) if the formation of image charge density proceeds on the time scale of the order of or longer than the pump–probe pulse duration and delay. In this regime a pump–probe experiment may yield information on the characteristics of such states rather than the states in relaxed image potential bands. Time scales of the various stages of these processes are estimated using an exactly solvable model of surface screening.

© 2010 WILEY-VCH Verlag GmbH & Co. KGaA, Weinheim

1 Early time interactions of quasiparticles excited at surfaces

The interpretation of excitation and detection of quasiparticles at surfaces in pump–probe experiments utilizing ultrashort laser pulses requires the assessment of quasiparticle dynamics and system relaxation from a true early evolution standpoint. While the non-adiabatic dynamics has been discussed in connection with the studies of surfaces and surface reactions by pulsed laser beams (for review see Refs. [1, 2]), the non-Markovian relaxation effects [3, 4] following optical excitation of surfaces have only recently become the subject of interest and theoretical modelling [5]. Here we shall discuss these effects on the example of two-photon-photoemission (2PPE) from paradigmatic systems whose initial ground state accommodates partly occupied quasi-two-dimensional surface state bands (Q2D SS-bands) on top of the bulk valence and conduction band structure [typically on (111) surfaces of Cu and Ag]. The discussion will be focused on electronic screening processes as the dominant relaxation mechanism and in this context on the dynamics of formation of the much discussed Q2D image potential band states (IS-states) that are observed in the surface projected band gaps between the vacuum level E_V and the Fermi energy E_F of the substrate [6]. These bands are not incorporated in the

initial equilibrium electronic structure because they arise as a result of the response of the system to introduction of electronic charge outside the surface.

In the initial step of 2PPE from surface bands [7] an electron excited out of the SS-band state by absorption of a pump pulse photon of energy $\omega_{pu} \leq E_V - E_F$ will first feel the initial state effective substrate potential and the interaction with unscreened SS-hole left behind. This leads to formation of a *coherent primary exciton* whose bound state discrete energy levels $E_l < E_V$ may form a Rydberg-like series characterized by the quantum numbers l that reflect the specificities of constrained electronic motion [8–10]. Subsequently, the two photocreated quasiparticles (SS-hole and excited electron) start interacting with the dynamical surface electronic response which will affect the amplitudes, energies and phases of primary excitonic states. As a result of these many-body interactions the primary states of excited quasiparticles will evolve in the course of time into a relaxed set of intermediate 2PPE states $\{|n\rangle\}$ that incorporate the effects of image screening in the form of developed image potential bands. The sequence of excitation and relaxation processes in the first stage of a 2PPE event induced by ultrashort pump pulse is illustrated schematically in the left-side panel of Fig. 1a.

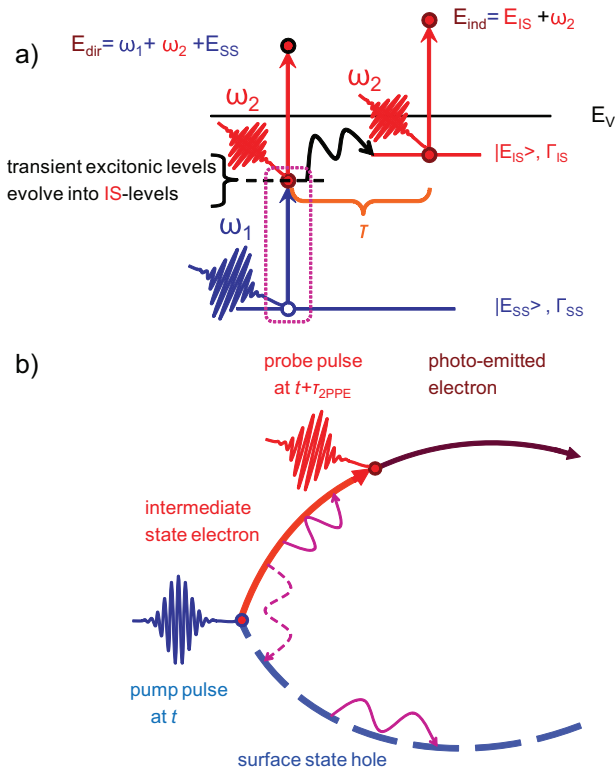


Figure 1 (online colour at: www.pss-b.com) (a) Illustration of the role of transient excitonic states as intermediate states in 2PPE from surface state band. The relaxation of transient excitonic states into image potential state(s) is denoted symbolically by a wiggly arrow. Variation of delay τ between two phase locked pulses may probe the relaxation of the physical basis set of intermediate states. (b) Diagrammatic illustration of the pump–probe photoexcitation process sketched in (a). Dashed and full lines denote the SS-hole and excited electron propagators, respectively. Dashed and full wavy lines denote the dynamically screened interactions involving bosonized electronic charge density fluctuations that contribute to the vertex and self-energy renormalizations of the skeleton diagram (cf. discussion in Section 4). Open end boson propagators describing excitation of real surface charge density fluctuations are not shown in the picture.

In the second stage of a 2PPE experiment the probe pulse photons eject electrons from the intermediate set of developed physical states (transient or relaxed) and thereby provide information on the excited state dynamics of the system (see right-side panel of Fig. 1a). The outgoing photoelectron states are due to their delocalization much less affected by the interaction with surface localized SS-hole than the intermediate states.

In order to understand the motivation for discussing relaxation processes in ultrafast 2PPE experiments it is important to observe that the many-body interactions which accompany evolution of the system from the initial excited state, over the transient excitonic states, to the relaxed states $\{|n\rangle\}$ that include the states of image potential bands, are not switched on adiabatically but rather instantaneously with the photoexcitation of primary electron–hole pair (e–h pair).

From the theoretical point of view this prevents the tracing of time-development operator back to early times ($t \rightarrow -\infty$) by using the adiabatic hypothesis on which the standard propagator techniques for descriptions of evolution of quasiparticles are based. A clear discussion of this principal issue was presented in Ref. [14].

In this paper we outline a model for description of temporal evolution and coherence of excited electron states at surfaces that reveals the most salient features of quasiparticle dynamics on the time scale typical of ultrafast pump–probe experiments. The model does not assume pre-existence of stationary image potential bands in the initial state but recovers them as a result of evolution of the excited system towards the screened state. On the basis of earlier studies of quasiparticle dynamics in surface bands [15–17] we expect that the electronic many-body relaxation processes will take place on the few femtosecond (fs) time scale. During this interval the dynamics of quasiparticles will be dominantly governed by coherent energy and amplitude relaxation because the irreversible decay of quasiparticles from quasistationary states may proceed and be traceable only after the formation of the latter.

2 Formulation of the model of unscreened surface exciton We start from a model in which prior to the photoexcitation of an e–h pair the many-electron system is described by one-electron eigenstates [18–21, 23] of the effective *initial* state (subscript ‘i’) one-particle Hamiltonian

$$H_i(\mathbf{p}, \mathbf{r}) = \frac{\mathbf{p}^2}{2m} + U_i(\mathbf{r}), \quad (1)$$

with the particle momentum $\mathbf{p} = (\hat{\mathbf{P}}, \hat{p}_z)$ and radiusvector $\mathbf{r} = (\mathbf{R}, z)$. Here bold capitals denote components of the operators and vectors in the lateral direction (i.e. parallel to the surface), and lower case italics the components in the z -direction perpendicular to the surface. The effective one-electron potential $U_i(\mathbf{r})$ is periodic in the lateral directions but for the sake of simplicity we shall assume in the following $U_i(\mathbf{r}) = U_i(z)$. This means that the effect of lateral periodicity will be accounted for through different effective electron ($m = m_e$) and hole mass ($m = m_h$) in the respective bands. Hence

$$H_i(\mathbf{p}, \mathbf{r}) = \frac{\hat{\mathbf{P}}^2}{2m} + \frac{\hat{p}_z^2}{2m} + U_i(z), \quad (2)$$

and the equation

$$H_i|\mathbf{K}, j\rangle = E_{\mathbf{K}, j}|\mathbf{K}, j\rangle = (\hbar^2\mathbf{K}^2/2m + \varepsilon_j)|\mathbf{K}, j\rangle, \quad (3)$$

yields the eigenenergies $E_{\mathbf{K}, j}$ and eigenstates $|\mathbf{K}, j\rangle$ of H_i , with \mathbf{K} and j denoting a 2D electron wavevector parallel to the surface and a quantum number describing electron motion perpendicular to the surface, respectively. In the following the energies $E_{\mathbf{K}, j}$ will be taken to describe the unperturbed *initial* state one-electron band structure.

In the forthcoming discussions we shall also refer to the *final* (subscript ‘f’) or relaxed one-particle Hamiltonian

$$H_f(\mathbf{p}, \mathbf{r}) = \frac{\mathbf{p}^2}{2m} + U_f(\mathbf{r}), \quad (4)$$

whose set of eigenstates includes also the image potential band states produced by the relaxation of effective surface potential when an electron is *adiabatically* brought to the surface [24]. Here we shall also assume $U_f(\mathbf{r}) = U_f(z)$. The set of eigenstates that diagonalize H_f is denoted by $\{|\mathbf{K}, n\rangle\}$ and their calculation was presented in Ref. [24], and in a slab model in Ref. [16]. Hence, the sets of one-electron states $|\mathbf{K}, j\rangle$ and $|\mathbf{K}, n\rangle$ that diagonalize H_i and H_f , respectively, are non-equivalent since they correspond to Hamiltonians with different effective one-particle potentials $U_i(z)$ and $U_f(z)$. An overview of the studies of many-body excitonic interactions in the models with $U_i(\mathbf{r}) = U_f(\mathbf{r})$ can be obtained from Refs. [10–13].

2.1 Primary surface exciton Hamiltonian For the convenience of forthcoming discussion we shall assume that the ground state of the system incorporates the states $|\mathbf{K}, j = \text{SS}\rangle$ of the SS-band because they represent an initial state feature pre-existent relative to the interactions switched on with optical excitation of the system. Together with the bulk states $|\mathbf{K}, j \neq \text{SS}\rangle$ they constitute a complete set of eigenstates that diagonalize H_i . It is this physical set of eigenstates occupied up to E_F in which individual electrons are ‘experimentally prepared’ before being exposed to the interaction with pulsed laser fields. In this simplified picture an excited e–h pair can be viewed as a two-body system described by the Hamiltonian [18, 20–22]

$$H_{2\text{body}}^{e-h} = H^e(\mathbf{p}_e, \mathbf{r}_e) + H^h(\mathbf{p}_h, \mathbf{r}_h) + V(\mathbf{r}_e - \mathbf{r}_h), \quad (5)$$

where $\mathbf{r}_{e,h} = (\mathbf{R}_{e,h}, z_{e,h})$ and $\mathbf{p}_{e,h} = (\mathbf{P}_{e,h}, p_{z:e,h})$ denote the electron (e) and hole (h) radius vectors and momenta, respectively. Here H^e and H^h are, respectively, one-particle Hamiltonians of the form (2) for the excited electron and hole which propagate in different bands, and

$$V(\mathbf{r}_e - \mathbf{r}_h) = -\frac{e^2}{|\mathbf{r}_e - \mathbf{r}_h|} \quad (6)$$

is the yet *unscreened* two-body e–h Coulomb interaction that depends only on the relative coordinate $|\mathbf{r}_e - \mathbf{r}_h|$. In view of the below discussed relaxation processes and time scales on which they proceed, the pair interaction (6) becomes effective only after the excitation of e–h pair. In other words, in the present problem the two-body interaction (6) does not obey the adiabatic boundary conditions but rather is switched on suddenly with the creation of primary e–h pair over the initial ground state [25].

Exploiting the symmetry of the problem, the one-particle wavefunctions that diagonalize H^e and H^h on the right-hand-side (RHS) of Eq. (5) can be, respectively, given

in the form

$$\psi_{\mathbf{K}_e, j_e}(\mathbf{r}_e) = \langle \mathbf{r}_e | \mathbf{K}_e, j_e \rangle = e^{i\mathbf{K}_e \mathbf{R}_e} \phi_{j_e}(z_e), \quad (7)$$

$$\psi_{\mathbf{K}_h, j_h}(\mathbf{r}_h) = \langle \mathbf{r}_h | \mathbf{K}_h, j_h \rangle = e^{i\mathbf{K}_h \mathbf{R}_h} \phi_{j_h}(z_h). \quad (8)$$

These wavefunctions constitute a complete set of electron and hole states that may be used in construction of pair states for description of early exciton dynamics.

We assume that prior to photoexcitation the electron is in a surface state described by the wavefunction $\psi_{\mathbf{K}_e, \text{SS}}(\mathbf{r}_e) = \langle \mathbf{r}_e | \mathbf{K}_e, \text{SS} \rangle$. In optically pumped transitions absorption of a photon lifts an electron to a higher unoccupied state $|\mathbf{K}, j\rangle$, leaving a hole in the initial state $|\mathbf{K}, \text{SS}\rangle$. From that instant onward the dynamics of excited e–h pair is in the absence of *other* interactions described by the *primary* exciton Hamiltonian (5). However, the creation of two uncompensated charges at the surface, viz. an electron in the state $|\mathbf{K}_e, j\rangle$ and a hole in the state $|\mathbf{K}_h, \text{SS}\rangle = |-\mathbf{K}_e, \text{SS}\rangle$, also switches on the quasiparticle interactions with the charge density fluctuations in the metal. In the course of time this renormalizes the bare quasiparticle energies and dynamically screens out their mutual Coulomb interaction (6). This is illustrated schematically in Fig. 1b. To study temporal evolution of this process we first need a description of the primary excitonic states.

2.2 Primary exciton wavefunctions and energies To obtain the surface exciton wavefunctions at the instant 0^+ after its excitation, we observe that if the e–h interaction $V(\mathbf{r}_e - \mathbf{r}_h)$ in (5) were absent, the problem would be separable and the total e–h wavefunction given by a linear combination of the products of electron and hole wavefunctions (7) and (8). Since only the lowest lying levels of electronic bands are important for formation of excitonic states [20], we may for practical purposes assume a single excited state band produced by effective $U_i(z_e)$ above the surface projected bulk band gap around E_V . Then, the form of Hamiltonian (5) suggests in the first approximation the representation of early exciton wavefunction as described in Refs. [18–21] and adjusted to the present problem characterized by the parallel to the surface (lateral) translational invariance. By introducing the e–h pair lateral relative coordinates

$$\boldsymbol{\rho} = \mathbf{R}_e - \mathbf{R}_h, \quad \mathcal{R} = \frac{1}{2}(\mathbf{R}_e + \mathbf{R}_h), \quad (9)$$

and their conjugate 2D momentum operators

$$\mathcal{Q} = \frac{1}{2}(\mathbf{P}_e - \mathbf{P}_h), \quad \mathcal{P} = \mathbf{P}_e + \mathbf{P}_h, \quad (10)$$

and substituting them in (5), one finds following Ref. [18] the transformed Hamiltonian:

$$H = -\frac{\hbar^2}{2\mathcal{M}} \frac{\nabla_{\mathcal{R}}^2}{4} - \frac{\hbar^2 \nabla_{\rho}^2}{2\mathcal{M}} - \frac{\hbar^2}{2} \left(\frac{1}{m_e} - \frac{1}{m_h} \right) \nabla_{\rho} \nabla_{\mathcal{R}} - \frac{\hbar^2}{2m_e^*} \frac{\partial^2}{\partial z_e^2} + U_i(z_e) - \frac{\hbar^2}{2m_h^*} \frac{\partial^2}{\partial z_h^2} + U_i(z_h) - \frac{e^2}{\sqrt{\rho^2 + (z_e - z_h)^2}}, \quad (11)$$

where m_e and m_h are the effective masses of electron and hole for motion in lateral direction, respectively, and $\mathcal{M} = m_e m_h / (m_e + m_h)$ is the corresponding reduced mass of the pair. Now, since the total lateral momentum operator for e-h pair $\mathcal{P} = -i\hbar \nabla_{\mathcal{R}}$ commutes with (11), its eigenvector $\mathbf{P} = (\mathbf{K}_e + \mathbf{K}_h)$ is a constant of motion. Hence, the exciton eigenstate $|\mathbf{P}, l\rangle$ with lateral momentum $\hbar\mathbf{P}$ and exciton quantum number l (or a set of quantum numbers) can be expanded in unperturbed e-h pair wavefunctions composed of (7) and (8), viz.

$$|\mathbf{P}, l\rangle = \sum_{\mathbf{K}_e, \mathbf{K}_h, j} \mathcal{A}_{\mathbf{K}_e, j; \mathbf{K}_h, \text{SS}}^{P, l} |\mathbf{K}_e, j; \mathbf{K}_h, \text{SS}\rangle, \quad (12)$$

where $j = j_e$ ranges over the set of all empty eigenstates $\langle z_e | j \rangle$ of the initial Hamiltonian H_i . For reasons explained earlier the *final relaxed states of image potential bands do not enter this summation* because they do not constitute the basis of the initial ground state of the system. The energies of exciton bound states of interest, ε_l , should be sought as the eigenvalues of a two-body Hamiltonian (5). Now, in the transformed coordinates representation (11) the lateral momentum operator \mathcal{P} can be replaced by its eigenvalue \mathbf{P} and hence

$$H_{2\text{body}}^{e-h} |\mathbf{P}, l\rangle = E |\mathbf{P}, l\rangle. \quad (13)$$

Following the analogy with Refs. [18, 20] the solution of (13) should yield the exciton energies and wavefunctions. We note that in the case of 3D-spherical bands discussed in Refs. [18, 20] the exciton bound state energies acquire the Rydberg-like form $-E_R/l^2$ ($l \geq 1$) where $E_R = \mathcal{M}e^4/2\hbar^2$ is expressed through the reduced e-h mass \mathcal{M} appropriate to 3D bands. A restricted version of Hamiltonian (11) with $\mathbf{P} = 0$ and appropriate to description of excitons in narrow quantum wells was studied in Ref. [26]. In the present case and in the effective mass approximation for non-degenerate Q2D bands the exciton bound state energies should appear in a similar form [cf. Eqs. (10) and (30) in Ref. [18]], viz.

$$E_{P, l} = \frac{P^2}{2\beta} - \varepsilon_l, \quad (14)$$

where β is a function of effective masses of electrons and holes excited in unoccupied 2D j bands and SS-band, respectively, and ε_l denote bound state exciton energies. In a

two-band model the first term on the RHS of (14) reduces to $P^2/2(m_e + m_h)$.

In optical transitions the momentum of the absorbed photon is negligible and hence the total exciton momentum is zero, viz. $\mathbf{P} = \mathbf{K}_e + \mathbf{K}_h = 0$. Then the wavefunction describing a primary exciton produced by photoexcitation of an electron from the SS-band reads

$$\langle \mathbf{r}_e, \mathbf{r}_h | \mathbf{P}, l \rangle = \Psi_{P, l}(\mathbf{r}_e, \mathbf{r}_h) = \sum_j \phi_j(z_e) \phi_{\text{SS}}(z_h) \sum_{\mathbf{K}_e + \mathbf{K}_h = 0} e^{i(\mathbf{K}_e \mathbf{r}_e + \mathbf{K}_h \mathbf{r}_h)} \mathcal{A}_{\mathbf{K}_e, j; \mathbf{K}_h, \text{SS}}^{P, l}. \quad (15)$$

Prior to the restriction $\mathbf{P} = 0$, the second sum on the RHS of (15) represents a 2D Fourier transform of the wavepacket amplitude in the lateral momentum space of an exciton with total momentum $\hbar\mathbf{P}$, i.e. it gives the corresponding wavepacket in the (x, y) -coordinate space [19, 20]. In the special case of optically induced transitions for which $\mathbf{P} = 0$ this wavepacket reduces to the form

$$\Phi_{j, \text{SS}}^{P=0, l}(\rho) = \sum_{\mathbf{K}_e} e^{i\mathbf{K}_e \rho} \mathcal{A}_{\mathbf{K}_e, j; -\mathbf{K}_e, \text{SS}}^{P=0, l}. \quad (16)$$

In this limit the appropriate Hamiltonian for description of optically induced excitons is obtained from (11) with \mathcal{P} replaced by $\mathbf{P} = 0$, and reads

$$H_{P=0}^{(\text{exc})} = -\frac{\hbar^2 \nabla_{\rho}^2}{2M} + H_z^e(z_e) + H_z^h(z_h) + V_{e-h}(\rho, z_e, z_h), \quad (17)$$

where

$$H_z^e(z_e) = -\frac{\hbar^2}{2m_e^*} \frac{\partial^2}{\partial z_e^2} + U_i(z_e), \quad (18)$$

$$H_z^h(z_h) = -\frac{\hbar^2}{2m_h^*} \frac{\partial^2}{\partial z_h^2} + U_i(z_h), \quad (19)$$

$$V_{e-h}(\rho, z_e, z_h) = -\frac{e^2}{\sqrt{\rho^2 + (z_e - z_h)^2}}. \quad (20)$$

For non-zero and small \mathbf{P} the mixed third term on the RHS of (11) containing $\nabla_{\rho} \nabla_{\mathcal{R}}$ can under certain conditions be treated by perturbation theory following Ref. [18].

2.3 Approximate calculation of primary exciton wavefunctions An approximate solution to Eq. (17) may be obtained following the arguments of Refs. [27, 28] employed in the description of motion of electrons and holes in perturbed periodic fields. We now make use of the assumption that even in the presence of e-h interaction (6)

the effective potential $U_i(z_h)$ is strong enough to localize the hole in pre-existent SS-band within a narrow region (of the order of few atomic radii) at the surface, i.e. within the extension of surface state electron density $|\phi_{SS}(z)|^2$ where $\phi_{SS}(z) = \langle z|j = SS \rangle$ is the eigenstate of (19). This is analogous to the adiabatic limit Ansatz of Kohn and Luttinger [28] in which the z -component of hole motion is solved first. For the currently studied problem the pertinent solution was presented in Refs. [16, 17]. The adiabatic limit Ansatz suggests the introduction of an effective excited electron Hamiltonian

$$\begin{aligned} H_{p=0}^{(\text{eff})} &= -\frac{\hbar^2 \nabla_{\rho}^2}{2\mathcal{M}} + H_z^e(z_e) + V_{e-h}^{(\text{eff})}(\rho, z_e) \\ &= \mathcal{H}_0(\rho, z_e) + V_{e-h}^{(\text{eff})}(\rho, z_e), \end{aligned} \quad (21)$$

in which

$$V_{e-h}^{(\text{eff})}(\rho, z_e) = -e^2 \int dz_h \frac{|\phi_{SS}(z_h)|^2}{\sqrt{\rho^2 + (z_e - z_h)^2}}, \quad (22)$$

plays the role of ‘impurity potential’ exerted by the hole in a pre-existent SS-state on the excited electron located at (ρ, z_e) . The signature of the integrated out hole coordinate z_h appears in the anisotropy of $V_{e-h}^{(\text{eff})}(\rho, z_e)$ which asymptotically behaves as;

$$\lim_{r \rightarrow \infty} V_{e-h}^{(\text{eff})}(\rho, z_e) = -\frac{e^2}{r} - \frac{e^2 z_e \bar{z}_h}{r^3} + \mathcal{O}(1/r^4), \quad (23)$$

where $r = \sqrt{\rho^2 + z_e^2}$ and $\bar{z}_h = \int z_h |\psi_{SS}(z_h)|^2 dz_h$ (note that a similar argument was employed in Ref. [26] to obtain an effective potential governing exciton dynamics in narrow quantum wells). Thereby the Schrödinger equation with Hamiltonian (21) expressed in the coordinates (ρ, z_e) becomes equivalent to the donor state wavefunction equation (3.1) of Ref. [28]. In the extreme limit in which $|\phi_{SS}(z_h)|^2$ is replaced by the density of a fixed point charge, the formation of the screening cloud on ultrashort time scale was studied in Ref. [29].

At this stage it is convenient to invoke the effective mass theory of Ref. [28] and apply it to (21) to obtain quantitative estimates of the primary exciton energy levels and wavefunctions. The solution follows the well known variation-of-constant method. We first assume that the unperturbed z -component $H_z^e(z_e)$ of (17) gives rise to electron band gap extending several eV below E_V and to a band (or bands) above the gap whose states near the bottom are non-degenerate. Next we assume that the effective e–h potential (22) gives rise to bound states that have dimensions large in comparison with the lattice period in the lateral directions so as that the conditions are fulfilled for writing the wavefunction of (21) in the form analogous to that discussed in Ref. [28] and appropriate to the present boundary conditions

$$\Psi(\rho, z_e) = F(\rho, z_e) \psi_j(\mathbf{K}_0, \rho, z_e). \quad (24)$$

Here $\psi_j(\mathbf{K}_0, \rho, z_e) = u(\mathbf{K}_0, \rho) \phi_j(z_e)$ is the unperturbed wavefunction describing electron at the bottom ($\mathbf{K} = \mathbf{K}_0$) of the j th band of $\mathcal{H}_0(\rho, z_e)$ of Eq. (21). The role of z -component of the band bottom wavefunction $\phi_j(z_e)$ is taken up by the lowest energy wavefunction of $H_z^e(z_e)$, Eq. (18), in the j th band. If the surface projected band gap straddles the vacuum level, then far outside the surface this eigenstate tends asymptotically to the vacuum energy wavefunction.

$F(\rho, z_e)$ satisfies the effective mass equation

$$\begin{aligned} \left[-\frac{\hbar^2 \nabla_{\rho}^2}{2\mathcal{M}} - \frac{\hbar^2}{2m_e^*} \frac{\partial^2}{\partial z_e^2} + V_{e-h}^{(\text{eff})}(\rho, z_e) \right] F(\rho, z_e) \\ = \varepsilon F(\rho, z_e), \end{aligned} \quad (25)$$

where m_e^* is the effective mass for electron motion in the z -direction near the j th band bottom of $H_0(\rho, z_e)$ defined in (21) which fixes the zero of ε . Thereby the effect of $U_i(z_e)$ on the electron motion is absorbed in m_e^* and the form of wavefunction $\psi_j(k_0, \rho, z_e)$. In the above described approximation the total exciton wavefunction corresponding to Hamiltonian (17) is obtained as a product of (24) and $\phi_{SS}(z_h)$.

The effective potential $V_{e-h}^{(\text{eff})}(\rho, z_e)$ is generally anisotropic as signified by expression (23) and illustrated in Fig. 2. Equation (25) is analogous to Eq. (3.4) of Ref. [28] and its solution may be attempted by several methods. Here we present the results of numerical solutions of Eq. (25) for Cu(111) surface obtained for few lowest bound state energy levels ε_l by using the DVR MCTDH and Fourier Grid Hamiltonian methods. The parameters used are $\mathcal{M} = 0.33$,

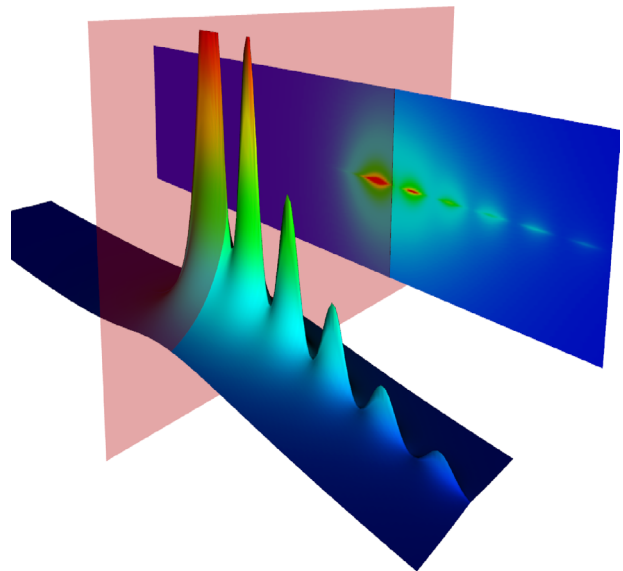


Figure 2 (online colour at: www.pss-b.com) Three dimensional contour plot illustrating the anisotropy of the modulus of effective potential $|V_{e-h}^{(\text{eff})}(\rho, z_e)|$ [cf. Eq. (22)] in the case of Cu(111) surface. Positive direction of the z -axis (i.e. exterior of the metal) is on the LHS of the picture. Light shaded sheet denotes the first surface plane of the crystal occupying the region of the viewer.

$m_e^* = 1$, and ε_l 's are measured from the relevant j th band bottom. We find:

$$\begin{aligned} \varepsilon_0(t = 0^+) &= -3.1961 \text{ eV} \\ \varepsilon_1(t = 0^+) &= -1.9516 \text{ eV} \\ \varepsilon_2(t = 0^+) &= -1.2928 \text{ eV} \\ \varepsilon_3(t = 0^+) &= -1.1261 \text{ eV} \\ \varepsilon_4(t = 0^+) &= -0.9634 \text{ eV} \\ \varepsilon_5(t = 0^+) &= -0.7730 \text{ eV} \\ \varepsilon_6(t = 0^+) &= -0.7271 \text{ eV, etc.} \end{aligned} \quad (26)$$

This substantiates the possibility of existence of excitonic precursor states in the intermediate stage of a 2PPE process. These ε_l are also in good semiquantitative agreement with the results obtained for transient excitons in bulk Cu [10]. Of course, for $t > 0$ the excitonic energy levels will vary in time following to the dynamics of screening of the bare e-h potential and the formation of quasiparticle-surface image potential (see Section 4). Here it is interesting to note that final bound state energy levels of the image potential [24] derived from (4) are nearly degenerate with higher ε_l listed in (26).

3 Population of primary excitonic levels induced by ultrashort pump pulses

The wavefunction prerequisites established in the preceding section enable us to estimate the evolution of optically induced populations of the primary states of transient surface excitons. The desired information is contained in quantum mechanical amplitudes $a_{l,SS}^P(t')$ describing these processes, i.e. the coefficients of the components of exciton wavefunctions obtained from first order time-dependent perturbation theory applied to electron interaction with the pump laser field [32]. Hence, the transition amplitudes appear linear and the populations quadratic in the field strength E . In the considered process an electron makes a transition from the initial state $|\mathbf{K}_e, SS\rangle$ into one of the $|\mathbf{K}_e, j\rangle$ states that constitute the (P, l) -th excitonic state (15). Making use of the above expressions we find that the probability amplitude pertaining to optically induced transition into excitonic state $|\mathbf{P} = 0, l\rangle$ is given by a coherent sum over j -bands:

$$\begin{aligned} a_{l,SS}^{P=0}(t') &= \sum_j D_{j,SS} e^{-iE_{P=0,l}t'} \Phi_{j,SS}^{P=0,l}(\boldsymbol{\rho} = 0) \\ &\times \frac{1}{i} \int_{-\infty}^{t'} dt_1 \mathcal{E}_{pu}(t_1) e^{i(E_{P=0,l} - \varepsilon_{SS})t_1}, \end{aligned} \quad (27)$$

where $D_{j,SS} = \boldsymbol{\mu}_{j,SS} \mathbf{E} = \langle \mathbf{K}_e, j | \mathbf{r}_e \mathbf{E} | \mathbf{K}_e, SS \rangle$ is the one-electron dipole matrix element, $\Phi_{j,SS}^{P=0,l}(\boldsymbol{\rho} = 0)$ is obtained from (16), and $\mathcal{E}_{pu}(t_1)$ is the modulation of pump pulse electromagnetic field. Assuming rotating wave approximation and Gaussian profile $G(t_1)$ of the pump pulse with carrier frequency ω_{pu} , viz. $\mathcal{E}_{pu}(t_1) = G(t_1) e^{-i\omega_{pu}t_1}$, we find that the integration on the RHS of (27) can be readily carried out. The conservation of energy in a single optically induced transition (i.e. in the absence of the probe pulse) is established in the limit $t' \rightarrow \infty$ taken in the integral on the

RHS of (27). On the other hand, in pump-probe induced transitions typical of 2PPE the conservation of energy sets in only after the completion of interactions with both laser fields. Mathematically this means after additional integration over the duration of interaction with the probe field $\mathcal{E}_{pr}(t')$, viz. $\int_{-\infty}^{t'} dt' \mathcal{E}_{pr}(t') \dots$, and letting $t \rightarrow \infty$.

Temporal variation of the probability of electronic transitions induced by an ultrashort Gaussian pulse from the occupied part of SS-band into l -th excitonic level is given by the absolute square of expression (27). This is illustrated in Fig. 3 for the case of Cu(111) surface (cf. this dependence with the ones shown Figs. 2a and 6a in Ref. [11]). It is seen that the pumping of a *single* excitonic level is a smooth process largely determined by the pulse duration. However, the population of final 2PPE states proceeding from excitonic levels may exhibit interference effects arising in the coherent sum of coefficients (27) over the manifold $\{|l\rangle\}$ of excitonic states.

4 Surface exciton in the presence of dynamical image screening

We shall describe the effects of dynamical screening at the surface within linear response formalism. This is equivalent to bosonization of the interaction of individual charges with the electronic charge density fluctuations in the system. The procedure is based on the observation that within linear response formalism the propagator of electronic charge density fluctuations can be conveniently represented by an equivalent boson propagator with the same excitation spectrum [16, 33]. The quantum numbers describing bosonized charge density excitations are their momentum \mathbf{Q} parallel to the surface and the excitation energy ω' . Thereby the dynamical screening effects are modelled by the interaction of charges of excited electron and hole with the boson field whose

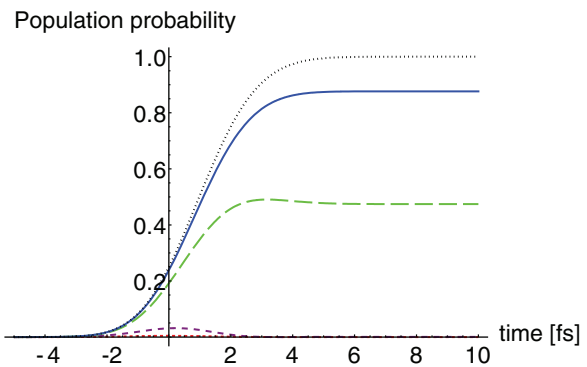


Figure 3 (online colour at: www.pss-b.com) Temporal variation of the relative population probabilities $|a_{l,SS}^{P=0}(t')|^2$ (normalized to respective $|D_{j,SS} \Psi_{j,SS}^{P=0,l}(\boldsymbol{\rho} = 0)|^2$) in electronic transitions from the SS-band on Cu(111) to four lowest stationary surface excitonic levels (26) detached from a single generic j th band (dotted, short dashed, long dashed and full curves, respectively), and to a resonant level $\varepsilon_{res} = \omega_{pu} + \varepsilon_{SS}$ (topmost dotted curve). The bottom of the j th band is taken to coincide with the vacuum level. Transitions are induced by ultrashort Gaussian pump pulse $G(t_1)$ centred around $t_1 = 0$, with carrier frequency $\omega_{pu} = 4.2 \text{ eV}$ and FWHM = 3 fs.

fluctuations are described by the linear electronic response function of the system. This passage was elaborated in Ref. [16] for the interaction of quasiparticles in surface bands with the substrate electronic response, and is shown schematically in Fig. 4 for the surface mediated component of the total e–h interaction discussed below.

We first outline a general framework for the description of coherent relaxation processes during which the energies of quasiparticles in non-stationary states are modified by their interactions with the developing electronic response of the system. Incoherent relaxation is usually associated with the quasiparticle recoil and irreversible decay out of the stationary states [16] and therefore can be well defined only upon the formation of the latter. We shall demonstrate that the action of coherent response can be modelled by an effective time-dependent potential which gives the leading contribution to surface mediated e–h interaction energy and is manifestly independent of the individual states of excited quasiparticles [34]. Our point of departure is the picture of screening of e–h potential (22) that is illustrated diagrammatically in Fig. 4. In this formulation the screening process is completely described by the full response function of the system, $\chi(\mathbf{r}_2, \mathbf{r}_1, t - t_1)$ elaborated in Ref. [16] and adapted to the present problem below. From this we may find the form of effective screened potential in the direct space as a function of the quasiparticle coordinates \mathbf{r}_e and \mathbf{r}_h or, by exploiting the translational symmetry along the surface, in the mixed space as a function of $(\mathbf{Q}, z_{e,h})$. Thereby we avoid preassumed states $|i\rangle$ in the formulation of early quasiparticle dynamics. In the field-theoretical description this corresponds to accounting for the renormalization of bare e–h interaction which becomes effective with the photoexcitation of the pair (cf. Fig. 1b).

Going over from space and time to the mixed (\mathbf{Q}, ω) -representation we may write for the total e–h interaction

$$V_{e-h}^{\text{tot}}(\mathbf{Q}, z_e, z_h, \omega) = V_{e-h}(\mathbf{Q}, z_e, z_h, \omega) + V_{e-h}^{(\text{ind})}(\mathbf{Q}, z_e, z_h, \omega). \quad (28)$$

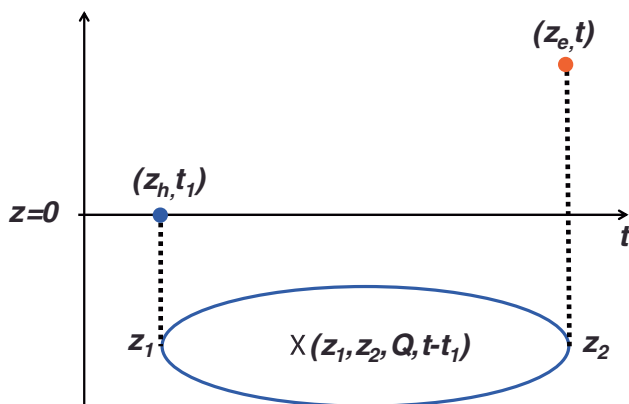


Figure 4 (online colour at: www.pss-b.com) Diagrammatic illustration of the screened component $\tilde{V}_{e-h}(\mathbf{Q}, z_e, z_h, t)$ of e–h interaction (31) for the case of hole charge density overlapping the substrate surface at $z = 0$.

Here $V_{e-h}(\mathbf{Q}, z_e, z_h, \omega)$ is the Fourier transform with respect to ρ and t of the suddenly switched on bare component of e–h potential $V_{e-h}(\rho, z_e, z_h)\Theta(t)$ with $V_{e-h}(\rho, z_e, z_h) < 0$ given by (20). In accord with this, the screened or polarization induced component of the total e–h interaction reads

$$V_{e-h}^{(\text{ind})}(\mathbf{Q}, z_e, z_h, \omega) = -\frac{i}{\omega + i\delta} \int dz_2 \int dz_1 V_Q e^{-Q|z_e - z_2|} \times \chi_Q(z_1, z_2, \omega) V_Q e^{-Q|z_1 - z_h|}. \quad (29)$$

The prefactor $i/(\omega + i\delta)$ is the Fourier transform of Heaviside step function, the minus sign in front arises from the attractive interaction between the positive hole charge and the electronic charge density fluctuations in the metal, and $V_Q = 2\pi e^2/Q$ is a 2D Fourier transform of the Coulomb interaction $e^2/|\mathbf{R}|$. We have omitted from expression (28) the unscreened e–h exchange interaction [12, 13] because its role in the discussed situation of surface bands with small spatial overlap was estimated to be of minor importance.

In the case when both the excited electron and the hole are localized well outside the surface and their charges have negligible overlap with the remaining electron density in the system, the exponential functions in the integrand of (29) factorize. This leads to the quantum analog of the classical image theorem [30, 16] that allows a simple definition of the surface response function in the exterior of the system (see next section). However, in a general situation of the holes excited in surface bands which overlap with the bulk electronic density and the image plane this is not the case. In this situation we must examine expression (29) in its general form to assess temporal evolution of the effective e–h potential. Since within the Kohn–Luttinger Ansatz [28] the hole motion is solved first, it is the temporal evolution of the hole density that causes the substrate charge density fluctuations which produce the induced potential (29). This imposes the use of retarded $\chi_Q(z_1, z_2, \omega)$ in the evaluation of (29). To this end we introduce the spectral representation

$$\chi_Q(z_1, z_2, \omega) = \int_0^\infty d\omega' \mathcal{D}_Q(z_1, z_2, \omega') \times \left(\frac{1}{\omega - \omega' + i\delta} - \frac{1}{\omega + \omega' + i\delta} \right), \quad (30)$$

and use it to calculate the Fourier transform of (29) which incorporates the time evolution of screened e–h interaction. Such a procedure yields a convolution of the suddenly switched on bare e–h potential [hence the appearance of the Fourier transform of the step function in (29)] with the response function χ , as it should within the linear response theory. This is shown schematically in Fig. 4 and in practice amounts to integrating $V_{e-h}^{(\text{ind})}(\mathbf{Q}, z_e, z_h, t - t_1)$ over t_1 constrained to the interaction interval $(0, t)$ [10]. This

produces a reactive (i.e. real or non-dissipative) retarded potential acting on the excited electron

$$\begin{aligned} \tilde{V}_{e-h}^{(\text{ind})}(\mathbf{Q}, z_e, z_h, t) &= \Theta(t) \int_0^t dt_1 V_{e-h}^{(\text{ind})}(\mathbf{Q}, z_e, z_h, t - t_1) \\ &= \Theta(t) \int dz_2 \int dz_1 V_{\mathbf{Q}}^2 e^{-Q|z_e - z_2|} e^{-Q|z_1 - z_h|} \\ &\quad \times \int_0^\infty d\omega' \mathcal{N}_{\mathbf{Q}}(z_1, z_2, \omega') (1 - \cos \omega' t), \end{aligned} \quad (31)$$

where $\mathcal{N}_{\mathbf{Q}}(z_1, z_2, \omega') = 2\mathcal{D}_{\mathbf{Q}}(z_1, z_2, \omega')/\omega'$. To further obtain the effective potential which the hole imparts on the electron in the approximation of frozen up hole wavefunction [28], the RHS of (29) is multiplied by the hole density $|\phi_{\text{SS}}(z_h)|^2$ and then integrated over z_h .

Several important general features of the dynamically screened e-h interaction can be readily deduced from expression (31). First, the induced potential (31) starts from zero at $t = 0$ and saturates for $t \rightarrow \infty$ at a finite value determined by

$$\begin{aligned} \tilde{V}_{e-h}^{(\text{ind})}(\mathbf{Q}, z_e, z_h, \infty) &= V_{\mathbf{Q}}^2 \int dz_2 \int dz_1 e^{-Q|z_e - z_2|} \\ &\quad \times \int_0^\infty d\omega' \mathcal{N}_{\mathbf{Q}}(z_1, z_2, \omega') e^{-Q|z_1 - z_h|}. \end{aligned} \quad (32)$$

This expression is analogous to and plays the role of the compressibility sum rule [31] or perfect screening sum rule [33] valid for probe charges residing in the interior or exterior relative to the surface, respectively. Its Fourier inversion into ρ -space yields the repulsive electron interaction with the electronic polarization cloud induced by the hole. Second, any prominent peak of non-negligible weight in the spectral density $\mathcal{N}_{\mathbf{Q}}(z_1, z_2, \omega')$ gives rise to attenuated oscillations of $\tilde{V}_{e-h}^{(\text{ind})}(\mathbf{Q}, z_e, z_h, t)$ around the saturation value, irrespective of the detailed structure of $\mathcal{N}_{\mathbf{Q}}(z_1, z_2, \omega')$. This will be illustrated in the next section in an exactly solvable model of screened surface exciton.

Expression (31) also enables the assessment of formation of the screening or image potential $\tilde{U}_e^{(\text{im})}(\mathbf{Q}, z_e, t)$ felt by an electron that is promoted at instant $t = 0$ to a distance z_e in the surface region. Following the above notation we find $\tilde{U}_e^{(\text{im})}(\mathbf{Q}, z_e, t) = -\frac{1}{2} \tilde{V}_{e-h}^{(\text{ind})}(\mathbf{Q}, z_e, z_e, t)$. This implies that the screening and attenuation of primary e-h excitonic potential and the formation of electron image potential proceed on the same pace because they are controlled by the same excitation spectrum $\mathcal{N}_{\mathbf{Q}}(z_1, z_2, \omega')$. This point will be further elaborated in the next section.

5 Exact model solution of the dynamics of exciton screening

5.1 Dynamical surface screening of e-h interaction

In order to learn about and understand better the physics of complex relaxation processes it is desirable to establish their descriptions within exactly solvable models whose solutions can be easily interpreted. A simple

illustration of the evolution of screening of e-h pair interactions at surfaces can be given for excited quasiparticles that have negligibly small overlap with the charge density inside the metal substrate (external exciton). A typical example of this case is photoexcitation from the states and/or orbitals localized outside the substrate image plane whose position is determined by the centroid of the induced charge density. This model is of great relevance despite its relative simplicity because linear response formalism provides exact description of screening of external perturbations owing to the validity of perfect screening sum rule [33] outside the image plane which defines the physical surface for electronic excitations. This situation also makes the application of Kohn-Luttinger approximation of quasistatic hole charge [28] well justified.

The above described conditions appear to be approximately satisfied on Ag(111) surfaces which support the surface state- and image potential state-bands. According to experimental evidence [35–37] all three low index surfaces of silver exhibit linear and positive (upward) surface plasmon dispersion, in contrast to the free-electron like metal surfaces for which it is negative and well described in jellium (Je) based models [38]. If, following the suggestions of Rocca et al. [37] and analyses of Feibelman [39], the bulk and surface plasmons in Ag are thought of as collective excitations split off the bottom of 4d–5s band of electron–hole excitations in the interior of the metal, then the position of the effective image plane will shift to the region of 4d orbitals, i.e. inward relative to the region of occupied surface and unoccupied image potential states that are localized outside the surface by the bulk band gaps. On the other hand, since small charge in SS-bands makes very small contribution to the response function (30), the relevant reference plane for SS-hole screening may be taken to be the same image potential plane that is shifted towards the interior by the presence of 4d-bands. Analogous arguments could also be extended to the Cu(111) surface (cf. Figs. 1 and 3 in Ref. [16] for the localization of SS- and IS-wavefunctions and for positive surface plasmon dispersion, respectively).

Within these boundary conditions the limit of (28) for z_e and z_h lying outside the image plane yields a selfconsistent e-h potential $V_{e-h}^{(\text{eff})}$ which in the (\mathbf{Q}, z, ω) representation takes the form [30, 33]

$$V_{e-h}^{(\text{eff})}(\mathbf{Q}, z_e, \omega) = V_{e-h}^{(\text{eff})}(\mathbf{Q}, z_e, \omega) + V_{e-h}^{(\text{im})}(\mathbf{Q}, z_e, \omega) R_{\mathbf{Q}}(\omega). \quad (33)$$

Here $V_{e-h}^{(\text{eff})}(\mathbf{Q}, z_e, \omega)$ is a 2D Fourier transform of e-h potential $V_{e-h}^{(\text{eff})}(\rho, z_e, t)$ of the type appearing on the LHS of Eq. (25). This is a definite approximation close to the image plane, but the one enabling good insight into underlying physics before the large scale computations based on expression (28) that describes a general situation are performed [47].

To derive the total potential (33) we first determine the bare e-h effective potential $V_{e-h}^{(\text{eff})}(\mathbf{Q}, z_e, \omega)$ and the polarization interaction $V_{e-h}^{(\text{im})}(\mathbf{Q}, z_e, \omega)$ from the (\mathbf{Q}, ω) -Fourier transforms of $V_{e-h}^{(\text{eff})}(\boldsymbol{\rho}, z_e, t) = V_{e-h}^{(\text{eff})}(\boldsymbol{\rho}, z_e)\Theta(t)$ and of $V_{e-h}^{(\text{im})}(\boldsymbol{\rho}, z_e, t) = V_{e-h}^{(\text{im})}(\boldsymbol{\rho}, z_e)\Theta(t)$, respectively (a more complicated time dependence of the interaction is briefly discussed at the end of this subsection). Note that $V_{e-h}^{(\text{eff})}(\boldsymbol{\rho}, z_e)$ is the same interaction that enters Eq. (25), and the interaction of the hole with the electron image is given by the image plane reflected expression [30]

$$V_{e-h}^{(\text{im})}(\boldsymbol{\rho}, z_e) = -e^2 \int dz_h \frac{|\phi_h(z_h)|^2}{\sqrt{\boldsymbol{\rho}^2 + (z_e + z_h)^2}}, \quad (34)$$

where $\phi_h(z_h)$ is here assumed to have negligible overlap with the substrate bulk wavefunctions. The remaining ingredient is the surface response function $R_{\mathbf{Q}}(\omega)$ obtained from $\chi_{\mathbf{Q}}(z_1, z_2, \omega)$ (cf. Appendix B in Ref. [16]) and expressed through its spectral representation [33]

$$R_{\mathbf{Q}}(\omega) = \int_0^\infty d\omega' \mathcal{S}_{\mathbf{Q}}(\omega') \times \left(\frac{1}{\omega - \omega' + i\delta} - \frac{1}{\omega + \omega' + i\delta} \right), \quad (35)$$

where $\mathcal{S}_{\mathbf{Q}}(\omega')$ is the spectral weight of surface electronic excitations of wavevector \mathbf{Q} and energy ω' .

Transforming the whole expression (33) back to real time representation and obeying the retarded character of the screening process as in Section 4, we find

$$V_{e-h}^{(\text{eff})}(\mathbf{Q}, z_e, t) = V_{e-h}^{(\text{eff})}(\mathbf{Q}, z_e)\Theta(t) - V_{e-h}^{(\text{im})}(\mathbf{Q}, z_e)\Theta(t) \times \int_0^\infty d\omega' N_{\mathbf{Q}}(\omega')[1 - \cos(\omega't)]. \quad (36)$$

Here $N_{\mathbf{Q}}(\omega') = 2\mathcal{S}_{\mathbf{Q}}(\omega')/\omega'$ plays the role of surface excitation spectrum that satisfies perfect screening sum rule $\int_0^\infty d\omega' N_{\mathbf{Q}=0}(\omega') = 1$ [33].

The second term on the RHS of (36) can be visualized as a FT of the (retarded) dynamic image mediated interaction between the photoexcited electron and hole at lateral separation $\boldsymbol{\rho}$. This is in full analogy with the screening of excitonic potentials in bulk systems [10] and it is gratifying that equivalent expressions (in terms of appropriate quantum numbers) are obtained in the interior and exterior regions of the dielectric. Hence, expression (31) intrapolates between the two limits across the atomically narrow interface. In the exterior the peculiar transient behaviour of the induced potential is governed by a transient factor in the second term on the RHS of (36), viz.

$$\mathcal{R}_{\mathbf{Q}}(t) = \int_0^\infty d\omega' N_{\mathbf{Q}}(\omega')[1 - \cos(\omega't)], \quad (37)$$

and analogously so in the interior of bulk systems (cf. Eq. (13) in Ref. [10]). Thereby the initial many-body problem of the reactive component of screening is formulated as an effective time-dependent one-electron potential problem. Transformation of (36) back into $\boldsymbol{\rho}$ -space and substitution into (25) in place of $V_{e-h}^{(\text{eff})}$ leads to a highly non-stationary one-particle time-dependent Schrödinger equation governing the evolution of excitonic wavefunction $F(\boldsymbol{\rho}, z_e, t)$. It should be noted that such a simple form of $\mathcal{V}^{(\text{eff})}(\mathbf{Q}, z_e, t)$ here follows from the assumption of sudden switching on of $V_{e-h}^{(\text{eff})}(\mathbf{Q}, z_e, t)$ and $V_{e-h}^{(\text{im})}(\mathbf{Q}, z_e, t)$ that both exhibit the time dependence $\propto \Theta(t)$, and the form of $R_{\mathbf{Q}}(t)$ employed in going from (33) to (36) prior to the treatment of quasiparticle recoil and decay from stationary states [16, 17, 34].

In order to demonstrate temporal evolution of the (dominant) long wavelength contribution to induced potential in (36) at real metal surfaces we shall use in (37) semi-empirical forms of the surface excitation spectra $\mathcal{S}_{\mathbf{Q}}(\omega')$ obtained earlier (cf. Fig. 1 in Ref. [40, 41] for Cu surface and Fig. 1 in Ref. [42] for Ag surface). The behaviour of $\mathcal{R}_{\mathbf{Q}=0}(t)$ for the case of electron promotion in front of Ag(111) and Cu(111) surfaces is illustrated in Fig. 5. It is seen that upon the excitation at $t=0$ the electron is solely affected by the bare potential $V^{(\text{eff})}(\mathbf{Q}, z_e)$ because $\mathcal{R}_{\mathbf{Q}}(t=0) = 0$, whereas after a sufficiently long interval [$t > 15$ fs for Ag(111) and $t > 3$ fs for Cu(111)] the total selfconsistent potential *saturates* and reaches the limit of the relaxed or screened potential

$$\mathcal{V}_{e-h}^{(\text{relax})}(\mathbf{Q}, z_e) = V_{e-h}^{(\text{eff})}(\mathbf{Q}, z_e) - V_{e-h}^{(\text{im})}(\mathbf{Q}, z_e). \quad (38)$$

One of the important messages conveyed by Fig. 5 is that due to the different electronic excitation spectra typifying the Ag(111) and Cu(111) surfaces the transient characteristics of image screening of e-h pair interactions at these surfaces are also notably different. In the case of Ag surface the image screening is dominantly governed by virtual excitations of surface plasmons of energy $\hbar\omega_s \simeq 3.8$ eV [42], whereas on Cu surface the screening process or the saturation of image charge is a much faster process because it is dominantly governed by higher energy interband excitations [40, 41].

A comparison of the time dependence in Fig. 3 with the ones shown in Fig. 5 indicates that on Cu(111) surface the population saturation of excitonic levels is an equally fast process as the renormalization of the e-h pair interaction by surface screening. On the other hand, on Ag(111) surface the saturation of population is a notably faster process than the screening of bare e-h interaction.

We may summarize the above findings by noting that the primary excitonic energy levels and wavefunctions will in the absence of other dynamical interactions evolve from the eigenvalues and eigenfunctions of (25) to less binding and more delocalized levels and wavefunctions determined by the screened e-h potential (38). It may also be observed that at large e-h separations the total static potential (38) acquires

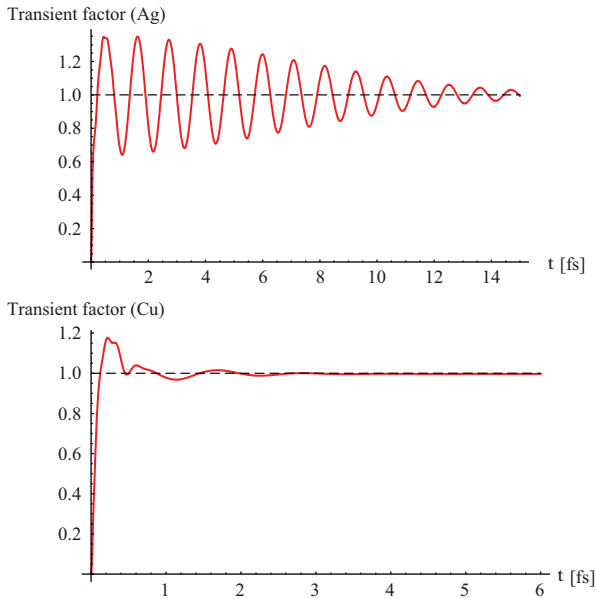


Figure 5 (online colour at: www.pss-b.com) Top panel: transient factor $R_{Q=0}(t)$ appearing in the second term on the RHS of (36) that determines evolution of the image component of e–h potential acting on the electron upon its promotion in front of Ag(111) surface. The transient oscillatory behaviour of image screening is caused by virtual excitation of surface plasmon which is a well defined excitation in this system (cf. surface excitation spectrum $S_Q(\omega')$ of Ag shown in Fig. 1 of Ref. [42]). Bottom panel: same for Cu(111) surface. Here the screening is much faster because it is dominated by higher energy interband transitions (cf. surface excitation spectrum $S_Q(\omega')$ of Cu shown in Fig. 1 of Ref. [41]).

a dipolar form:

$$\lim_{r \rightarrow \infty} \mathcal{V}_{e-h}^{(\text{relax})}(\boldsymbol{\rho}, z_e) = -\frac{2e^2 \bar{z}_h z_e}{r^3}, \quad (39)$$

with the strength determined by the image of hole dipole $-2e\bar{z}_h$ depending on the separation of hole density centre of mass \bar{z}_h from its image at $-\bar{z}_h$ [note the difference with respect to (23)].

Lastly, we observe that expression (33) offers a more general description of the screening of bare excitonic interaction. Since in the pump pulse-induced excitation of a primary e–h pair the hole is created in a pre-existent state its subsequent decay will cause a time dependent depletion of the initial hole charge density appearing in the integrand on the RHS of (22). This depletion process can be described by the hole survival probability $L_h(t)$ which for SS-band holes was elaborated in Refs. [16, 17]. Hence, replacing the Kohn–Luttinger frozen up hole density with the one described by the hole survival probability, the screening of e–h interaction may be described by a version of expression (33) in which the ω -dependence of the matrix elements $V_{e-h}^{(\text{eff})}$ and $V_{e-h}^{(\text{im})}$ is given by the Fourier transform of $L_h(t)\Theta(t)$ instead of the potential switching step function $\Theta(t)$ only. However, both

approaches require the solution of the same primary exciton problem.

The validity of the above arguments for the screening of e–h interaction outside the image plane should be also applicable without resorting to the effective e–h bare potential (22) in which the hole wavefunction is frozen up (i.e. treated adiabatically after the hole has been photo-excited). Following the analogy with expression (36) and without resorting to preassumed states, the time-dependent interaction between electron and hole point charges located at z_e and z_h outside the surface, respectively, can be written directly in the (\boldsymbol{Q}, z, t) -space in terms of the Coulomb matrix elements V_Q as

$$\mathcal{V}_{e-h}(\boldsymbol{Q}, z_e, z_h, t) = V_{e-h}(\boldsymbol{Q}, z_e, z_h)\Theta(t) + \tilde{V}_{e-h}^{(\text{im})}(\boldsymbol{Q}, z_e, z_h, t), \quad (40)$$

with

$$V_{e-h}(\boldsymbol{Q}, z_e, z_h) = -V_Q e^{-Q(|z_e - z_h|)}, \quad (41)$$

and

$$\tilde{V}_{e-h}^{(\text{im})}(\boldsymbol{Q}, z_e, z_h, t) = V_Q e^{-Q(|z_e| + |z_h|)} \Theta(t) \times \int_0^\infty d\omega' N_Q(\omega') [1 - \cos(\omega' t)], \quad (42)$$

and then transformed back into the $(\boldsymbol{\rho}, z)$ -space and the result substituted on the RHS of expression (17) to replace the bare (unscreened) e–h interaction. Thereby the problem of screened external exciton is modelled by a two-particle Hamiltonian involving a time-dependent interparticle potential.

5.2 Dynamical image screening of the excited electron and hole

Photoexcitation of an electron–hole pair in front of the surface also switches on individual interactions of constituent quasiparticles with the electronic response of the system. This induces dynamical image screening of each quasiparticle. In the present formulation of external excitons such processes can be treated on the same footing as the screening of e–h interaction discussed in Section 5.1. In the field-theoretical description these effects manifest themselves through the quasiparticle self-energy corrections [34]. Specifically, an electron excited in the region outside the surface image plane will experience its own quantum image potential which in the mixed $(\boldsymbol{Q}, z_e, \omega)$ -representation is given by [33]

$$U_e^{(\text{im})}(\boldsymbol{Q}, z_e, \omega) = U(\boldsymbol{Q}, -z_e, \omega) R_Q(\omega), \quad (43)$$

where $U(\boldsymbol{Q}, -z_e, \omega)$ is the (\boldsymbol{Q}, ω) -Fourier transform of the suddenly switched on Coulomb image potential $U(\boldsymbol{Q}, -z_e)$ for the electron located at $(\boldsymbol{\rho}, z_e)$. Following the arguments of Section 5.1, we find that the evolution of image potential is described by

$$U_e^{(im)}(\mathbf{Q}, z_e, t) = -U(\mathbf{Q}, -z_e)\Theta(t) \times \int_0^\infty d\omega' N_{\mathbf{Q}}(\omega') [1 - \cos(\omega't)]. \quad (44)$$

Note that this interaction is responsible for the evolution of unrelaxed initial set of eigenstates $|\mathbf{K}, j\rangle$ of H_i , over into the final set of relaxed eigenstates $|\mathbf{K}, n\rangle$ of H_f discussed in Section 2.1. A completely analogous procedure can be followed to obtain dynamical image potential $U_h^{(im)}(\mathbf{Q}, z_h, t)$ of the hole photoexcited outside the image plane.

We note in passing that in the present linear screening theory the long time limits of polarization mediated quasiparticle interactions derived in Sections 4 and 5 do not exhibit any Debye–Waller factor (DWF) type of renormalizations [44, 45]. This is in contrast to the quasiparticle propagators which exhibit the DWF effects upon renormalization by the interactions with the same bosonized polarization fields [5, 16].

5.3 Representation of exciton screening by an effective time-dependent two-body Hamiltonian The screening dynamics of e–h potential (36), as well as of the image potentials of external individual quasiparticles, is factorized from the matrix elements of bare interactions. These expressions may now be used in a simple modelling of the screening induced energy relaxation of an e–h pair photoexcited outside the surface image plane. In this picture the e–h interaction as well as the individual quasiparticle interactions with the surface response are represented by effective time-dependent potentials whose magnitudes are varying on the ultrashort time scale. Hence, to assess the temporal variation of primary excitonic energy levels we can formulate an effective two-body time-dependent excitonic Hamiltonian describing relaxation dynamics of an e–h pair subsequent to its optical excitation at, say, $t = 0$. This effective Hamiltonian takes the form

$$H_{P=0}^{\text{exc}}(t) = H_{P=0}^{\text{exc}} + V_{\text{tot}}^{(im)}(t) \quad (45)$$

with $H_{P=0}^{\text{exc}}$ given by expression (17), and

$$V_{\text{tot}}^{(im)}(t) = \tilde{V}_{e-h}^{(im)}(\boldsymbol{\rho}, z_e, z_h, t) + \frac{1}{2}U_e^{(im)}(\boldsymbol{\rho}, z_e, t) + \frac{1}{2}U_h^{(im)}(\boldsymbol{\rho}, z_h, t), \quad (46)$$

where the terms on the RHS of (46) are given by the $\boldsymbol{\rho}$ -Fourier transforms of the respective expressions in the \mathbf{Q} -space. At $t = 0$ expression (45) describes the primary exciton because $V_{\text{tot}}^{(im)}(t = 0) = 0$, and in the limit of full relaxation, $t \rightarrow \infty$, the Hamiltonian (45) tends to the expression given by Eq. (2) of Ref. [43]. This is illustrated in Fig. 6. It should be noted that the thus formulated time-dependent Hamiltonian (45) does not incorporate dissipative effects. The latter may be incorporated *a posteriori*

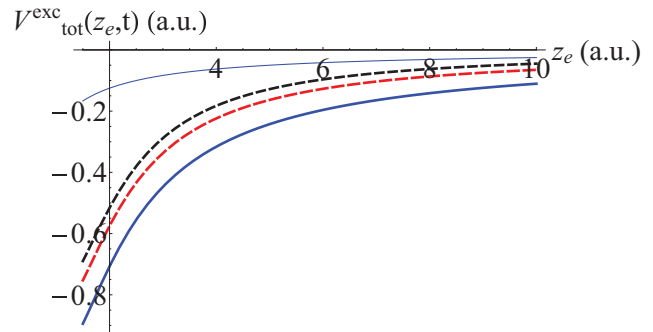


Figure 6 (online colour at: www.pss-b.com) Illustration of the temporal development of total time-dependent electron potential energy $V_{\text{tot}}^{\text{exc}}(\boldsymbol{\rho}, z_e, t) = \tilde{V}_{e-h}^{(im)}(\boldsymbol{\rho}, z_e, z_h, t) + 1/2U_e^{(im)}(\boldsymbol{\rho}, z_e, t)$ appearing on the RHS of expression (46) for the hole at 1 a.u. outside the image plane on Ag(111) surface and mutual e–h separation $\rho = 1$ a.u. Full line: $t = 0$ (primary excitonic potential). Long dashed line: $t = 2.25$ fs (combination of partly screened e–h and incompletely developed e-image potential energy contributions). Short dashed line: $t = \infty$ (fully relaxed electron potential energy with prevailing electron image contribution). The short dashed line reaches asymptotically (beyond $z_e = 10$ a.u. measured from the image plane) the classical electron image energy $-e^2/4z_e$ shown by the uppermost thin full line.

following the methods of Ref. [16] once the quasistationary state is reached.

The e–h dynamics governed by the effective Hamiltonian (45) can be visualized as the evolution of excited e–h pair that is initially dominated by interband e–h interaction which rapidly weakens due to dynamic screening. This gives way to the domination of individual interactions of quasiparticles with their developing screening charges as described by the last two terms on the RHS of (46). When the asymptotic limit of fully screened total interaction is reached (given by the sum of non-binding or very weakly binding e–h potential and fully developed electron and hole image potentials), the individual quasiparticle states will be well described by the final state one-particle Hamiltonian (4). In other words, the dynamics of excited e–h pairs evolves from propagation in early excitonic, strongly correlated states, over into the regime of electron and hole propagation in the states of developed IS-band and relaxed SS-band, respectively. In this context the relaxed electron image potential energies may be viewed as excitonic levels for which the role of ‘exciton hole’ has in the course of screening been taken from the SS-hole and transferred to the emergent electron image screening charge induced at the surface (i.e. to the excited electron’s exchange correlation hole). Once the stationary state of the electronic system described by the eigenstates of (4) has been attained, the electron decoherence and decay from stationary states may be described by the formalisms of Refs. [16, 17, 46].

6 Discussion of the dynamics of transient excitonic states The above developed model description

of screening of quasiparticles at surfaces provides basic insight into the early evolution of energetics of intermediate electronic states probed in time and energy resolved pump–probe investigations of the surface electronic structure and dynamics. It is argued that in the case of pump–probe spectroscopies of occupied surface bands on Cu(111) and Ag(111) surfaces the pump-induced primary electronic transitions can be viewed as creation of transient excitonic states whose energy levels lie in the surface projected band gaps. The subsequent evolution of primary excitonic levels is governed by the dynamics of screening processes at the surface. Reactive (i.e. non-dissipative) interactions of photoexcited quasiparticles with the developing screening charge renormalize the initial bare e–h interaction and give rise to the formation of relaxed image potential bands in concurrent processes.

This approach offers a dynamical picture of the intermediate states and energy levels in pump–probe spectroscopies of surface bands. These levels arise as bound states of the effective time dependent potential (46) which due to dynamical screening evolves from the initial excitonic potential dominated by the unscreened Coulomb attraction of photoexcited SS-hole over into the relaxed or saturated image potential caused by the screening charge developed at the surface. In that sense both the primary excitonic states and the relaxed image potential states can be viewed as bound excitonic states of a potential that is initially governed by the SS-hole and finally by the exchange-correlation hole (i.e. image charge) of individual quasiparticles. In the Kohn–Luttinger approximation [28] employed in Section 2.3 to calculations of primary excitonic levels this implies diabatic transitions $\varepsilon_i(t \rightarrow \infty) \rightarrow \varepsilon_n$ where ε_n are energies of image potential states calculated in Ref. [24]. A general formulation of the relaxation dynamics of excitonic states based on the surface response outlined in Section 4 will be further elaborated elsewhere [47].

To facilitate discussions of the characteristics of transient excitonic states we introduced in Section 5 a simplified, yet highly illustrative model of screening of e–h pairs excited outside the substrate surface. This constraint on quasiparticle charge distributions allows closed form representations of the interactions which drive the primary excitonic states into the states of relaxed image potential. Special merit of this approach lies in easy visualisation of the dynamics of transient excitonic states at surfaces, and thereby of the role these states may play in ultrafast pump–probe experiments. Although the validity of solutions of such a simplified model is restricted to exterior of the image plane, the general physical implications deriving thereof should be extendable beyond the regions of formal applicability of the model itself. Thus we find that the screening of bare e–h pair interaction outside the image plane and the formation of individual quasiparticle image potentials proceed at the common pace. On Ag(111) the relaxation during which transient excitons fade and the image potential bands are being formed is completed within an interval of the order of ~ 15 fs, whereas on the Cu(111) this time is much shorter, of

the order of ~ 3 fs (cf. Fig. 5). This strong difference arises from the markedly different structures of surface electronic excitation spectra which govern the dynamics of screening at respective substrate surfaces. In the spirit of Section 2 this can be rephrased in that the evolution of effective one-particle Hamiltonians H_i into H_f is a much faster process on Cu(111) than on Ag(111) surface.

We have also investigated the role of ultrashort pump pulse duration on the dynamics of population of primary excitonic states. For the parameters characteristic of the studied systems and the currently available ultrashort laser pulses of FWHM ~ 3 fs which may still provide required resolution in interferometric experiments [1, 48], the saturation of population of a primary excitonic level occurs in the interval of ~ 4 – 5 fs. This is comparable to the duration of formation of image potential bands on Cu(111) surface and means that for pump–probe delays exceeding this time the probe pulse would measure occupation of the states in the already relaxed image potential bands, with all the implications regarding the existence of well defined intra- and inter-band transitions among the stationary states deriving from the relaxed $H_{P=0}^{\text{exc}}(t \rightarrow \infty)$, the ensuing non-adiabatic and dissipative processes governing the decay rates and lifetimes of excited states, etc. On the other hand, in the case of Ag(111) surface the required interval may exceed ~ 15 – 18 fs because of a much slower screening of excitonic interaction and saturation of the image potential. That altogether permits longer duration of transient excitonic states and slower formation of image potential bands.

The third factor which limits direct observation of the ‘standard’ features of quasiparticles in ultrafast experiments, viz. their energy and exponential decay governed by lifetime effects, is the early evolution of quasiparticles after being promoted into the established or pre-existent quasistationary states. According to our recent calculations [16, 17, 46] the Markovian regime of exponential decay and phase saturation of quasiparticles in surface bands on Cu(111) is reached within first 6–7 fs after the photoexcitation. This imposes pump–probe delays which exceed that interval, otherwise the transient, early excited particle features are likely to be detected.

The effects of ultrafast excitation and relaxation processes outlined above will effectively appear convoluted in the amplitudes of 2PPE events, viz. integrated over all intermediate times in the diagrams of the form illustrated in Fig. 1b. Therefore, in order to assess quasiparticle energies and lifetimes in relaxed quasistationary states, the delay time between the applied pump and probe pulses should exceed the three discussed temporal intervals. On the other hand, for shorter delays the experiment may detect non-relaxed or transient intermediate states, in particular on the Ag(111) surface. The latter system poses a challenge to possible detection of transient excitonic and early quasiparticle states as intermediate states in time resolved 2PPE and interferometric 2PPE + 1PPE experiments [1, 48]. One of the goals of the present discussion is to motivate such

experiments and the development of a unified theory for their interpretation.

Note added in proof: Recent measurements have provided evidence for positive (upward) surface plasmon dispersion also on Au(111) surface [49]. Hence, the model of dynamical screening of “external exciton” outlined in Section 5 should be applicable to this surface as well.

Acknowledgements This work has been supported in part by the Ministry of Science, Education and Sports of the Republic of Croatia through the Research Projects nos. 035-0352828-2839, 098-0352828-2863 and 098-0352851-2921.

References

- [1] H. Petek and S. Ogawa, *Prog. Surf. Sci.* **56**, 239 (1997); H. Petek and S. Ogawa, *Annu. Rev. Phys. Chem.* **53**, 507 (2002).
- [2] Ch. Frischkorn and M. Wolf, *Chem. Rev.* **106**, 4207 (2006).
- [3] R. Kubo, M. Toda, and N. Hashitsume, *Statistical Physics II, Nonequilibrium Statistical Mechanics* (Springer-Verlag, Berlin Heidelberg, 1998), Ch. 3.
- [4] S. M. Almoudi, D. Boyanovsky, and H. J. de Vega, *Phys. Rev. E* **60**, 94 (1999).
- [5] For short review of these effects see: P. Lazić, D. Aumiler, and B. Gumhalter, *Surf. Sci.* **603**, 1571 (2009).
- [6] For reviews of relaxed electronic structure of surface bands see: P. M. Echenique, R. Berndt, E. V. Chulkov, Th. Fauster, A. Goldman, and U. Höfer, *Surf. Sci. Rep.* **52**, 219 (2004); E. V. Chulkov, A. G. Borisov, J. P. Gauyacq, D. Sánchez-Portal, V. M. Silkin, V. P. Zhukov, and P. M. Echenique, *Chem. Rev.* **106**, 4160 (2006), and references therein.
- [7] For review of the theory of 2PPE from surfaces see: H. Ueba, and B. Gumhalter, *Prog. Surf. Sci.* **82**, 193 (2007).
- [8] X.-F. He, *Phys. Rev. B* **43**, 2063 (1991).
- [9] B. Gumhalter, *Surf. Sci.* **518**, 81 (2002).
- [10] W.-D. Schöne and W. Ekardt, *Phys. Rev. B* **62**, 13464 (2000).
- [11] D. B. Tran Thoai and H. Haug, *Phys. Rev. B* **47**, 3574 (1993).
- [12] W. Hanke and L. J. Sham, *Phys. Rev. B* **21**, 4656 (1980).
- [13] A. Marini and R. Del Sole, *Phys. Rev. Lett.* **91**, 176402 (2003).
- [14] M. Wagner, *Phys. Rev. B* **44**, 6104 (1991).
- [15] F. El-Shaer and B. Gumhalter, *Phys. Rev. Lett.* **93**, 236804 (2004).
- [16] P. Lazić, V. M. Silkin, E. V. Chulkov, P. M. Echenique, and B. Gumhalter, *Phys. Rev. B* **76**, 045420 (2007).
- [17] P. Lazić, V. M. Silkin, E. V. Chulkov, P. M. Echenique, and B. Gumhalter, *Phys. Rev. Lett.* **97**, 086801 (2006).
- [18] G. Dresselhaus, *J. Phys. Chem. Solids* **1**, 14 (1956).
- [19] G. Dresselhaus, *Phys. Rev.* **106**, 76 (1957).
- [20] R. J. Elliott, *Phys. Rev.* **108**, 1384 (1957).
- [21] R. J. Elliott, in: *Polarons and Excitons*, Scottish Universities' Summer School 1962, edited by C. G. Kuper and G. D. Whitfield (Plenum Press, New York, 1963), p. 269.
- [22] R. Zimmermann, *Phys. Status Solidi B* **173**, 129 (1992).
- [23] M. Rohlfing, N.-P. Wang, P. Krüger, and J. Pohlmann, *Phys. Rev. Lett.* **91**, 256802 (2003).
- [24] N.-P. Wang, M. Rohlfing, P. Krüger, and J. Pohlmann, *Phys. Rev. B* **67**, 115111 (2003).
- [25] E. V. Chulkov, V. M. Silkin, and P. M. Echenique, *Surf. Sci.* **437**, 330 (1999).
- [26] P. Nozières and C. T. De Dominicis, *Phys. Rev.* **178**, 1097 (1969).
- [27] O. Betbeder-Matibet, M. Combescot, and C. Benoit à la Guillaume, *Phys. Status Solidi B* **213**, 33 (1999).
- [28] J. M. Luttinger and W. Kohn, *Phys. Rev.* **97**, 869 (1955).
- [29] W. Kohn and J. M. Luttinger, *Phys. Rev.* **98**, 915 (1955).
- [30] A. Borisov, D. Sánchez-Portal, R. Díez Muiño, and P. M. Echenique, *Chem. Phys. Lett.* **387**, 95 (2004).
- [31] D. M. Newns, *Phys. Rev. B* **1**, 3304 (1970).
- [32] D. Pines and P. Nozières, *The Theory of Quantum Liquids*, Vol. I (Benjamin, New York and Amsterdam, 1966), Ch. 2. p. 3.
- [33] For pulse characterizations see: K. Boger, M. Roth, M. Weinelt, Th. Fauster, and P.-G. Reinhard, *Phys. Rev. B* **65**, 075104 (2002).
- [34] B. Gumhalter, *Prog. Surf. Sci.* **15**, 1 (1984), Sections 2 and 3.
- [35] C. H. Hodges, *J. Phys. C, Solid State Phys.* **8**, 1849 (1975).
- [36] R. Contini and J. M. Layet, *Solid State Commun.* **64**, 1179 (1987).
- [37] M. Rocca and U. Valbusa, *Phys. Rev. Lett.* **64**, 2398 (1990).
- [38] M. Rocca, M. Lazzarino, and U. Valbusa, *Phys. Rev. Lett.* **69**, 2122 (1992).
- [39] K.-D. Tsuei, E. W. Plummer, A. Liebsch, E. Pehlke, K. Kempa, and P. Bakshi, *Surf. Sci.* **247**, 302 (1991).
- [40] P. J. Feibelman, *Surf. Sci.* **282**, 129 (1993).
- [41] D. Lovrić and B. Gumhalter, *Phys. Rev. B* **38**, 10323 (1988).
- [42] D. Lovrić and B. Gumhalter, *Surf. Sci.* **287/288**, 789 (1993).
- [43] D. Lovrić, B. Gumhalter, and K. Wandelt, *Surf. Sci.* **307–309**, 953 (1994).
- [44] C. Benoit à la Guillaume, M. Combescot, and O. Betbeder-Matibet, *Solid State Commun.* **108**, 193 (1998).
- [45] B. Gumhalter, *Surf. Sci.* **347**, 237 (1996).
- [46] A. Šiber and B. Gumhalter, *Phys. Rev. Lett.* **90**, 126103 (2003).
- [47] B. Gumhalter, A. Šiber, H. Buljan, and Th. Fauster, *Phys. Rev. B* **78**, 155410 (2008).
- [48] B. Gumhalter, P. Lazić, N. Došlić, E. V. Chulkov, and V. M. Silkin, unpublished.
- [49] J. Güdde, M. Rohleder, T. Meier, S. W. Koch, and U. Höfer, *Science* **318**, 1287 (2007).
- [50] S. J. Park and R. E. Palmer, *Phys. Rev. Lett.* **102**, 216805 (2009).